

AD-763 886

CHARACTERIZATION OF EMP PROTECTION
DEVICES

G. G. Davidson, et al

Army Electronics Command
Fort Monmouth, New Jersey

July 1973

DISTRIBUTED BY:

NTIS

National Technical Information Service
U. S. DEPARTMENT OF COMMERCE
5285 Port Royal Road, Springfield Va. 22151

AD



Research and Development Technical Report
ECOM- 4128

AD 763886

CHARACTERIZATION OF EMP PROTECTION DEVICES

G. G. Davidson
E. T. Hunter

NATIONAL TECHNICAL
INFORMATION SERVICE

July 1973

DISTRIBUTION STATEMENT
Approved for public release
distribution unlimited

ECOM

UNITED STATES ARMY ELECTRONICS COMMAND · FORT MONMOUTH, N.J.

Reports Control Symbol OSD-1366

TECHNICAL REPORT ECOM-4138

CHARACTERIZATION OF EMP PROTECTION DEVICES

By

G. G. DAVIDSON

E. T. HUNTER

Semiconductor Devices & Integrated Electronics Technical Area
US Army Electronics Technology and Devices Laboratory (ECOM)

ADDITIONAL

DA Work Unit No. 196 62705 A 440 01 321

Distribution Statement

Approved for public release; distribution unlimited.

US ARMY ELECTRONICS COMMAND
FORT MONMOUTH, NEW JERSEY

ABSTRACT

Since late 1969, a technique based on time domain reflectometry (TDR) to measure the fast switching and shunting capability of EMP protective devices has been used. This technique allows the devices to be characterized in their actual working condition--inserted in the cable line--without the perturbing influence of voltage and current probes.

This report starts with the basic line theory and develops an understanding of the effect of shunt devices and the measurement of such effects using TDR. This section is fairly lengthy; however, a good background is essential for the understanding of measurements made with this technique.

In addition to the measurement technique itself, a special pulse generator was developed to provide the necessary pulse into 50Ω lines. This pulse source is described along with the basic measurement procedure. Specific techniques and data are shown for a variety of shunt protective devices.

UNCLASSIFIED

Security Classification

DOCUMENT CONTROL DATA - R & D

(Security classification of title, text of Abstract and text of Executive Summary shall be shown even when the overall report is classified)

1. ORIGINATING ACTIVITY (Corporate author) US Army Electronics Command Fort Monmouth, New Jersey 07703	2a. REPORT SECURITY CLASSIFICATION Unclassified 2b. GROUP
--	--

3. REPORT TITLE
CHARACTERIZATION OF EMP PROTECTION DEVICES

4. DESCRIPTIVE NOTES (Type of report and inclusive dates)
Technical Report

5. AUTHOR(S) (First name, middle initial, last name)
G. G. Davidson
E. T. Hunter

6. PERIODICITY	7a. TOTAL NO. OF PAGES 403	7b. NO. OF PAGES
----------------	--------------------------------------	------------------

8a. CONTRACT NUMBER	9. DOWNGRADING REPORT NUMBER EXOM-
---------------------	--

8b. CONTRACT ELEMENT	9. OTHER REPORT NUMBER (Any other numbers that may be assigned this report)
----------------------	---

10. STATEMENT OF AVAILABILITY
Approved for public release; distribution unlimited.

11. SUPPLEMENTARY NOTES Let us know if you wish to study on microfiche.	12. SPONSORING/MONITORING AGENCY NAME(S) AND ADDRESS(ES) US Army Electronics Command ATTN: AMSEL-TL-IR Fort Monmouth, New Jersey 07703
--	---

13. ABSTRACT

Since late 1959, a technique based on time domain reflectometry (TDR) to measure the fast switching and shunting capability of EMP protective devices has been used. This technique allows the devices to be characterized in their actual working conditions--inserted in the cable line--without the perturbing influence of voltage and current probes.

This report starts with the basic line theory and develops an understanding of the effect of shunt devices and the measurement of such effects using TDR. This section is fairly lengthy; however, a good background is essential for the understanding of measurements made with this technique.

In addition to the measurement technique itself, a special pulse generator was developed to provide the necessary pulse into 50 ohm lines. This pulse source is described along with the basic measurement procedure. Specific techniques and data are shown for a variety of shunt protective devices.

UNCLASSIFIED

Security Classification

14 KEY WORDS	LINK A		LINK B		LINK C	
	ROLE	WT	ROLE	WT	ROLE	WT
EMP Protection Protective Devices Time Domain Reflectometry						

HLSA FM 1092-73

10

Security Classification

CONTENTS

	<u>Page</u>
1. INTRODUCTION	1
2. THEORY	1
3. EXPERIMENTAL	11
a. Pulse Generator	11
b. Measurement Technique	12
4. RESULTS	14
a. Zener Diodes	15
b. Four-Layer Diodes/Silicon Controlled Rectifiers	17
c. Spark Gaps	18
d. Spark Gap (Special Screw Type)	21
e. Neon Bulbs	21
5. CONCLUSIONS	22
a. Measurement Technique	22
b. Protection Device Characteristics	22
6. ACKNOWLEDGMENTS	22

TABLE

I. Definition of Symbols	2
--------------------------	---

FIGURES

1. Fast Pulser	11
2. Pulse Measurement Block Diagram	12
3. Single Point Measurement Block Diagram	13
4. Voltage Amplitude Vs. Firing Time of Spark Gap	14
5. Voltage Transmitted Past Zener Diode 1N3026B	17

6.	Input and Transmitted Signals for a Four-Layer Diode	17
7.	Transmitted Signal for a Four-Layer Diode Shunting a 4 kV Step	18
8.	Spark Gap and Nearby Low Impedance Load	19
9.	Transmitted Signal Spark Gap UBD550	19
10.	Transmitted Voltage for Signalite Spark Cap	20
11.	Transmitted Signal for Special Screw Type Spark Cap	21
12.	Voltage Transmitted Past 90 V Neon Bulb	21

APPENDIX

I.	List of Source and Transforms	23
II.	List of Network Function Transforms (Special Case for $Z_0 = \infty \Omega$)	25
III.	Signal Transform by Linear Approximation and Derivatives	27
IV.	Equation Solution by Convolution	30
V.	Example of Measurements and Calculations	35

CHARACTERIZATION OF EMI PROTECTION DEVICES

1. INTRODUCTION

Nuclear weapon detonations can generate electric and magnetic pulse (EMP) fields capable of disabling military electronic equipments. Military communication-electronic systems are particularly vulnerable to pulse energy coupled into antennas and input cables. The protection of these systems against the EMP may be accomplished by use of devices which shunt this pulse energy away from the sensitive parts of the system.

Because of the high voltage and the fast rise time nature of the pulses being dealt with, the standard data provided by manufacturers give little indication of just how well a device will shunt the pulse energy. Contributing to the actual device response is the added impedance of the package and leads, all very important at these pulse frequencies. Since late 1960, a technique based on time domain reflectometry (TDR) to measure the fast switching and shunting capability of a variety of potential protective devices has been used. Samples of spark gaps, four-layer diodes, silicon controlled rectifiers (SCR), neon bulbs, and zener diodes were measured and the resulting data analyzed.

The characteristics of the high voltage and fast rise time pulse were such that there was no generator available for bench top testing. This requirement led to the development of a pulse generator to provide the necessary pulses.

In order to fully understand this measurement technique and the resulting data, a little background in line theory and pulse response is included in this report along with sample results showing its application.

2. THEORY

In this section and in the several appendices to the report, the background theory of TDR techniques as applied to pulse measurements is developed. Special cases are examined as they apply to overall understanding. Table I is a glossary of the symbols used throughout the report and is provided because the selection of subscripts is not standardized in the current literature.

For the case under consideration, that of shunt type devices, line theory gives the relation between the voltage transmitted, E_T , and the voltage reflected, E_R , in terms of the line characteristics for a given input voltage, E_{IN} . Line characteristics include characteristic impedance, Z_0 , and termination.

TABLE I. DEFINITION OF SYMBOLS

<u>SYMBOL</u>	<u>DEFINITION</u>
E_{IN}	Voltage In
E_R	Voltage Reflected
E_T	Voltage Transmitted
E_L	Voltage Across Load
P_{IN}	Power In on Line
P_R	Power Reflected
P_L	Power to Load
P_D	Power to Device
P_T	Power Transmitted Down Line
Z_0	Characteristic Impedance
Z_D	Impedance of Shunt Device
Z_L	Impedance of Total Load
Y_0	Characteristic Admittance
Y_L	Admittance of Load
Y_T	Admittance of Network to be Protected
Y_D	Admittance of Device
$\rho(s)$	Reflection Coefficient
$M(s,$	Transmission Coefficient
$s)$	Fourier transform (frequency domain)

$$E_T(s) = |1 + \rho(s)| E_{IN}(s) = M(s) E_{IN}(s)$$

and

$$E_R(s) = \rho(s) E_{IN}(s)$$

where

$$\rho(s) = \frac{Z_L(s) - Z_0}{Z_L(s) + Z_0}$$

and

$$M(s) = 1 + \rho(s)$$

The impedances are complex, and the voltages are transformed into the s-domain.

The corresponding power relationships are also shown as follows:

$$\begin{aligned} P_D = P_R + P_L &= \frac{E_R^2}{Z_0} + \frac{E_T^2}{Z_L} = \frac{E_{IN}^2}{Z_0} \\ &= \frac{(\rho E_{IN})^2}{Z_0} + \frac{(1 + \rho)^2 E_{IN}^2}{Z_L} \\ &= \rho^2 \frac{E_{IN}^2}{Z_0} + \frac{(1 + \rho)^2}{\left(\frac{1 + \rho}{1 - \rho}\right)} \frac{E_{IN}^2}{Z_0} \end{aligned}$$

$$\therefore P_R = \rho^2 P_{IN}$$

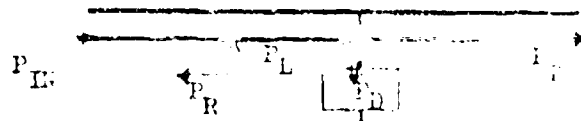
$$\text{and } P_L = (1 - \rho^2) P_{IN}$$

The power delivered to the load, P_L , is a combination of the power delivered to the shunt device, P_D , and the power transmitted past the protective device, P_T .

$$P_L = P_D + P_T$$

Similarly, the admittances are related

$$Y_L = Y_D + Y_T$$



Beyond the protective device may be found the protected circuit, a 500 load, a long line, an oscilloscope or any combination of these, and Y_T represents the total admittance of the combination. For the special case of a long line only beyond the protective device,

$$Y_T = Y_0$$

and

$$P_L = P_D + P_T = E_L^2 Y_D + E_L^2 Y_0$$

Also,
$$P_L = (1 - \rho^2) P_{IN}$$

and

$$P_L = (1 + \rho)^2 E_{IN}^2 Y_L$$

therefore,

$$P_L = (1 + \rho)^2 E_{IN}^2 Y_D + (1 + \rho)^2 E_{IN}^2 Y_0$$

$$P_D = (1 + \rho)^2 E_{IN}^2 Y_D$$

$$= (1 + \rho)^2 E_{IN}^2 Y_D \cdot \frac{Y_0}{Y_0}$$

$$= (1 + \rho)^2 \frac{Y_D}{Y_0} P_{IN}$$

But, P_D also equals P_L minus P_T :

$$P_D = P_L - P_T$$

$$= (1 - \rho^2) P_{IN} - (1 + \rho)^2 P_{IN}$$

$$= -2\rho(1 + \rho) P_{IN}$$

P_D is positive, since from our original definition of ρ we can show that

$$\rho = - \frac{1}{1 + 2 \frac{Y_0}{Y_D}}$$

for this special case in which $Y_T = Y_0$.

From this very basic introduction, examination of specific characteristics of a shunt protective device can begin. It is assumed that such a device, although non-linear, has two unique states and can, thus, be represented by two specific impedances. The switching transients associated with the transfer between these two states are considered insignificant when compared to the transients introduced by the forcing function. In general, when such a device is in its shunt mode, it appears as a small resistor and series inductor across the transmission line, so that

$$Z_L = R_L + j X_L$$

and

$$Z_{Y,} \left| \begin{array}{l} t \rightarrow \infty \\ s \rightarrow 0 \end{array} \right. = R_L$$

and

$$\rho = \frac{R_L - R_0}{R_L + R_0}$$

If it is assumed that, while conducting, $R_L \ll R_0$, then $\rho \approx -1$ and

$$P_R = \rho^2 P_{IN} \quad \text{which}$$

indicates that almost all of the input power is reflected back from the protective device.

In order to determine approximate values of the power absorbed and that reflected from the protective device, let us assume that the line is terminated by the device and that $P_T = 0$. Then

$$\begin{aligned} P_L = P_D &= (1 - \rho^2) P_{IN} \\ &= (1 + \rho)(1 - \rho) P_{IN} \end{aligned}$$

$$= M(1 - \rho) P_{IN}$$

$$M = 1 + \frac{R_L - R_0}{R_L + R_0} = \frac{2 R_L}{R_L + R_0}$$

but $R_0 \gg R_L$, and $M \approx \frac{2 R_L}{R_0}$

$$(1 - \rho) = 1 - \frac{R_L - R_0}{R_L + R_0} = \frac{2 R_0}{R_L + R_0}$$

again, $R_0 \gg R_L$, so that $(1 - \rho) \approx 2$. Therefore,

$$P_D \approx 2 \left(\frac{2 R_L}{R_0} \right) P_{IN} = 4 \frac{R_L}{R_0} P_{IN}$$

Similarly,

$$P_R \approx \left(1 - \frac{4 R_L}{R_0} \right) P_{IN}$$

If no protection device were present, the preceding formulation could represent the power absorbed and reflected from a termination device such as a forward biased transistor or diode.

Examination of further types of terminations will provide a better understanding of effects on unprotected devices and circuits. In the following section there is no protection device, i.e., $Y_D = 0$.

a. Resistive Termination

In this case, $Z_L = R_L$ and ideally the reflection coefficient is given by:

$$\rho(s) = \frac{R_L - Z_0}{R_L + Z_0}$$

and the transmission coefficient is given by:

$$M(s) = \frac{2 R_L}{R_L + Z_0}$$

From the equation for power delivered to a load,

$$P_L = (1 - \rho^2) P_{IN}$$

it can easily be shown that for a shorted line ($R_L = 0$), $P_L = 0$; for an open line ($R_L = \infty$), $P_L = 0$; and for a line terminated in its characteristic impedance ($R_L = Z_0$), $P_L = P_{IN}$.

b. Reactive Termination

In this case, the transmitted and reflected voltages will be displaced in time from the input voltage. The best way to demonstrate this is by considering an inductor shunting, not terminating, an ideal transmission line, and using an input step voltage:

$$E_{IN}(t) = E_{IN} u(t)$$

and its Laplace transform

$$E_{IN}(s) = \frac{E_{IN}}{s}$$

$$\rho(s) = \frac{Y_0 - Y_L}{Y_0 + Y_L} = \frac{Z_L - Z_0}{Z_L + Z_0}$$

where $Y_L = Y_0 + Y_{INDUCTOR}$

$$\therefore \rho(s) = - \frac{1}{1 + 2 \frac{Y_0}{Y_{INDUCTOR}}} = - \frac{1}{1 + 2 \frac{Z_{INDUCTOR}}{Z_0}}$$

and

$$M(s) = \frac{2 \frac{Z_{INDUCTOR}}{Z_0}}{1 + 2 \frac{Z_{INDUCTOR}}{Z_0}}$$

If the line is purely resistive ($Z_0 = R$) and the inductor has no resistive component ($Z_{INDUCTOR} = sL$), then

$$E_R(s) = - \left(\frac{1}{1 + \frac{2sL}{R}} \right) \frac{E_{IN}}{s}$$

$$= \frac{R}{2L} \left| \frac{1}{s \left(s + \frac{R}{2L} \right)} \right| R_{IN}$$

and by Laplace transform:

$$E_R(t) = \left(\frac{R}{2L} \right) (1 - e^{-\frac{R}{2L}t}) E_{IN} u(t)$$

and

$$E_T(t) = e^{-\frac{R}{2L}t} E_{IN} u(t)$$

This is the common method of obtaining the reflected and transmitted time responses. Laplace transforms of various source functions are given in Appendix I and the transforms of various transmission line shunt elements are given in Appendix II.

The experimental measurement of $E_{IN}(t)$, $E_R(t)$, and $E_T(t)$ by observing the reflected pulse at the input point is confounded by normal line loss. An imperfect transmission line will degrade both the amplitude and shape of the pulse. Calibration of the system using known terminating conditions is therefore a requirement.

Another point of concern is the effect of changing the characteristic impedance of the transmission line. For a device inserted in a long transmission line,

$$D(s) = \frac{-Y_D}{2Y_0 + Y_D}$$

and

$$N(s) = \frac{2Y_0}{2Y_0 + Y_D}$$

Therefore,

$$E_T = \frac{1}{1 + \frac{Y_D}{2Y_0}} E_{IN} = \frac{1}{1 + \frac{Z_0}{2Z_D}} E_{IN}$$

If $Z_0 \gg 2Z_D$, then

$$E_T \approx \frac{2Z_D}{Z_0} \cdot E_{IN}$$

Therefore, a larger Z_0 reduces the output voltage for the same device impedance. One problem with using higher characteristic impedance transmission lines is that the device insertion loss under dc conditions is greater for the same device impedance. Consider the 3 dB fall-off point for a device behaving like a capacitor under normal signal conditions:

$$Z_D \approx X_C = \frac{1}{j\omega C}$$

$$\text{at 3 dB fall-off, } \left| \frac{Z_0}{2} \right| \approx \left| Z_D \right| = \left| \frac{1}{j\omega C} \right|$$

If C is fixed, then

$$\omega = \frac{1}{\frac{Z_0}{2} \cdot C}$$

and it can be seen that, as the characteristic impedance is increased to increase the reflection coefficient for a large pulse, the advantage may be offset by the lower frequency drop-off under normal signal conditions.

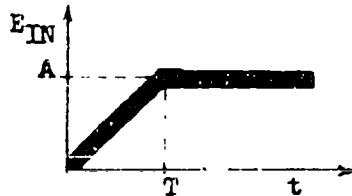
Suppose that we have a transmission line with a shunting device which appears as a resistor and an inductor in series, and we want to know the equivalent R and L values. Again,

$$\rho(s) = \frac{Z_L - Z_0}{Z_L + Z_0} \quad \text{where } Z_L = R + sL$$

and

$$M(s) = 2 \left(\frac{s + \frac{R}{L}}{s + \frac{1}{\tau}} \right) \quad \text{where } \tau = \frac{L}{R + R_0}$$

Let us assume a source voltage of amplitude A and wave shape shown below.



The transform of this source function is given by:

$$E_{IN}(s) = \left(\frac{A}{T} \right) (1 - e^{-sT}) \left(\frac{1}{s^2} \right)$$

The voltage passing the shunt is given by:

$$\begin{aligned} E_T(s) &= M(s) E_{IN}(s) \\ &= 2 \left(\frac{s + \frac{R}{L}}{s + \frac{1}{\tau}} \right) \left(\frac{A}{T} \right) \left(\frac{1}{s^2} \right) (1 - e^{-sT}) \\ &= 2 \left(\frac{A}{T} \right) (1 - e^{-sT}) \left[\frac{s + \frac{R}{L}}{s^2 \left(s + \frac{1}{\tau} \right)} \right] \end{aligned}$$

Expanding,

$$E_T(s) = \left(\frac{A}{T} \right) 2 (1 - e^{-sT}) \left[\frac{-\tau^2 \frac{R}{L} + \tau}{s} + \frac{\tau \frac{R}{L}}{s^2} + \frac{\tau^2 \left(\frac{R}{L} - \frac{1}{\tau} \right)}{s + \frac{1}{\tau}} \right]$$

and its inverse transform:

$$I_T(t) = 2 \left(\frac{A}{T} \right) \left\{ \left[\left(\tau - \frac{R}{L} \tau^2 \right) + \frac{R}{L} \tau t + \tau^2 \left(\frac{R}{L} - \frac{1}{\tau} \right) e^{-\frac{t}{\tau}} \right] u(t) - \left[\left(\tau - \frac{R}{L} \tau^2 \right) (1 - e^{-\frac{t-T}{\tau}}) + \frac{R}{L} \tau (t-T) \right] u(t-T) \right\}$$

If we let $s \rightarrow 0$, and take the limit of $sE_T(s)$, we find that

$$E_T \Big|_{s \rightarrow 0} = 2 A \frac{R}{L}$$

and, since $\tau = \frac{L}{R + R_0}$ and $E_{IN} \Big|_{t \rightarrow \infty} = A$

$$E_T \Big|_{t \rightarrow \infty} = 2 E_{IN} \left(\frac{R}{R + R_0} \right)$$

Solving for R,

$$R = \frac{R_0 E_T}{2 E_{IN} - E_T}$$

Thus, a measurement of E_T at long times allows calculation of R.

Knowing the value of R, the value of L can be obtained by further calculation as follows, since the maximum value of E_T occurs when $t = T$.

$$\begin{aligned} E_T(\max) &= 2 \left(\frac{A}{T} \right) \left[\left(\tau - \frac{R}{L} \tau^2 \right) + \frac{R}{L} \tau T + \tau^2 \left(\frac{R}{L} - \frac{1}{\tau} \right) e^{-\frac{T}{\tau}} \right] \\ &= 2 \left(\frac{A}{T} \right) \left[\frac{R}{L} \tau T + \tau \left(1 - \frac{R}{L} \tau \right) \left(1 - e^{-\frac{T}{\tau}} \right) \right] \\ &= 2 A \left(\frac{R}{R + R_0} \right) \left[1 + \frac{1}{T} \frac{R_0}{R} \left(1 - e^{-\frac{T}{\tau}} \right) \right] \end{aligned}$$

Assuming that $R \ll R_0$, and that $T \gg \tau$:

$$E_T(\max) \approx 2 A \frac{1}{T} = 2 \left(\frac{A}{T} \right) \frac{L}{R_0}$$

and $\frac{A}{T}$ is the slope of the input voltage function.

Solving for L: -

$$L = \frac{E_{T(\max)} \cdot R_0}{2 \left(\frac{A}{T}\right)}$$

This equation represents a coil shunting a transmission line. The series L, R combination is a bit more difficult, but it may be obtained from the original $E_{T(\max)}$ equation.

Alternatively, L can be determined by further experimental measurements, e.g., by measuring the actual decay of the pulse, the time constant can be obtained. (We define τ , the circuit time constant, as the time between the beginning of pulse decay and the 50% decay point, divided by 0.693.) Then,

$$L = (R + R_0) \tau$$

Or, even simpler, substitute series combinations of R and various inductors until the same output and/or reflected voltage is obtained.

3. EXPERIMENTAL

a. Pulse Generator. A pulse generator has been designed to simulate an EMP induced pulse as it would appear at the end of a cable. Pulse characteristics were selected based on limited experimental evidence and some assumptions. The resulting pulse should more than adequately evaluate the usefulness of the various shunt type protective devices. Figure 1 shows the finished pulser along with its circuit diagram and typical output pulse.

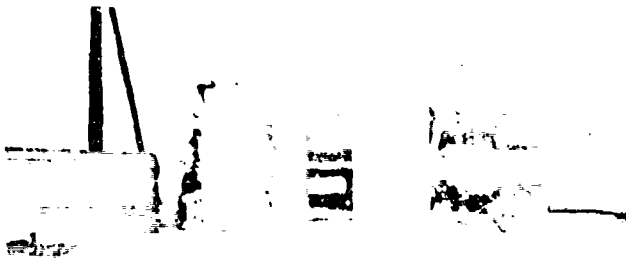


Fig. 1a

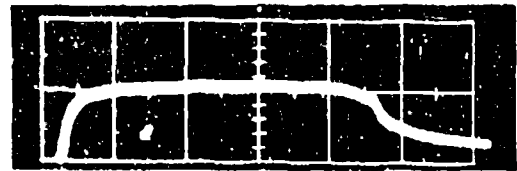


Fig. 1b
h-50 ns/cm v-4000 V/cm

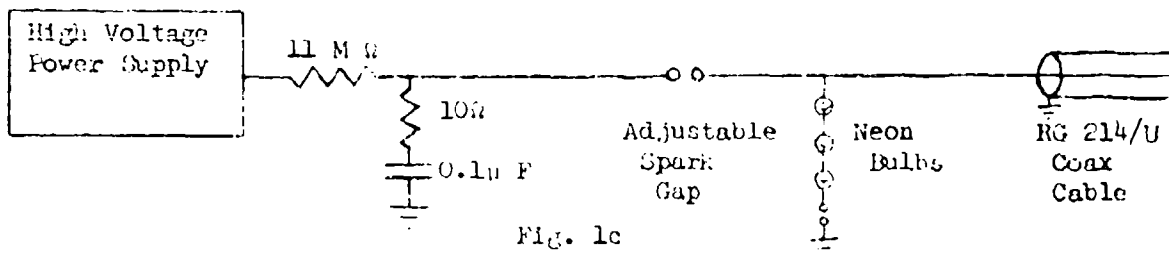


Fig. 1c

FIG. 1. Fast Pulser

The high voltage supply charges the 0.1 μ F capacitor through the 11 M Ω resistor, which determines the firing rate. The voltage on the capacitor increases until the first spark gap breaks down. Then, the chain of neon bulbs ignite and the second spark gap breaks down. The width of the first gap and the charging voltage determine the breakdown voltage and, therefore, the output pulse amplitude. The pulse width is determined by the delay in firing the chain of neon bulbs, and the second gap produces the sharp fall time of the pulse. Pulse rise time is a function of the first gap characteristic, circuit inductance, and internal inductance of the capacitor.

Characteristics obtainable with this pulse include a rise time less than 15 ns and pulse duration from 20 to 1000 ns at magnitudes up to 4000 V. The pulser is capable of supplying 8000 V for 150 ns into a 50 Ω line. The pulse generator can be operated in a single shot mode by swinging an insulator into the first gap after it fires, but before it can fire a second time. The repetition rate can be made very low by varying the charging circuit time constant and the width of the first gap.

Since the majority of protection devices under investigation are triggered into the shunt mode at voltages below 2000 V, the linearity of the initial pulse slope (200 V/ns maximum) is sufficient to measure rise time effects on most devices.

b. Measurement Technique. The basic measurement requires observation of both the injected pulse and the transmitted pulse. A reflected pulse will be seen at the same point where the injected pulse is observed but delayed according to the length of transmission line. A separate measurement of the transmitted pulse is needed because of its nature and magnitude. Figure 2 shows a block diagram of this standard set up.

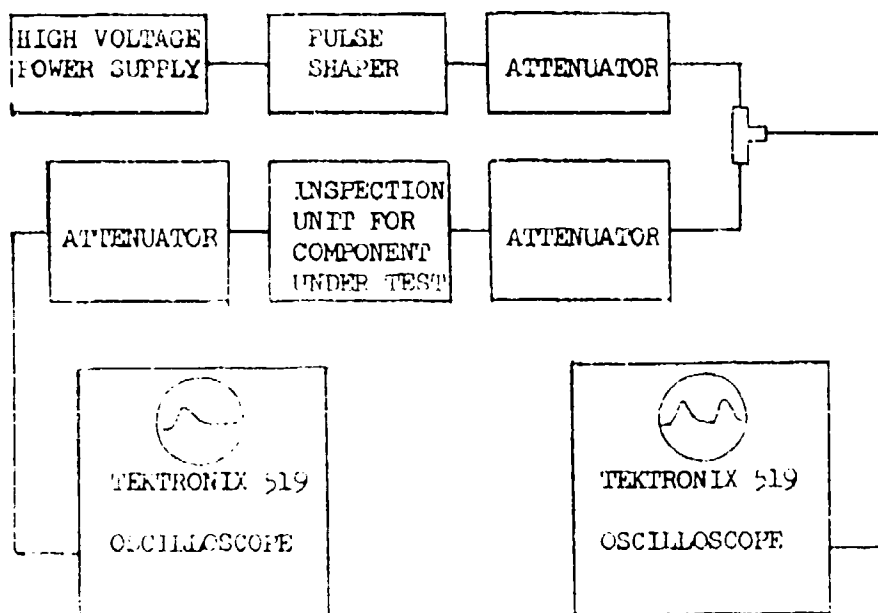
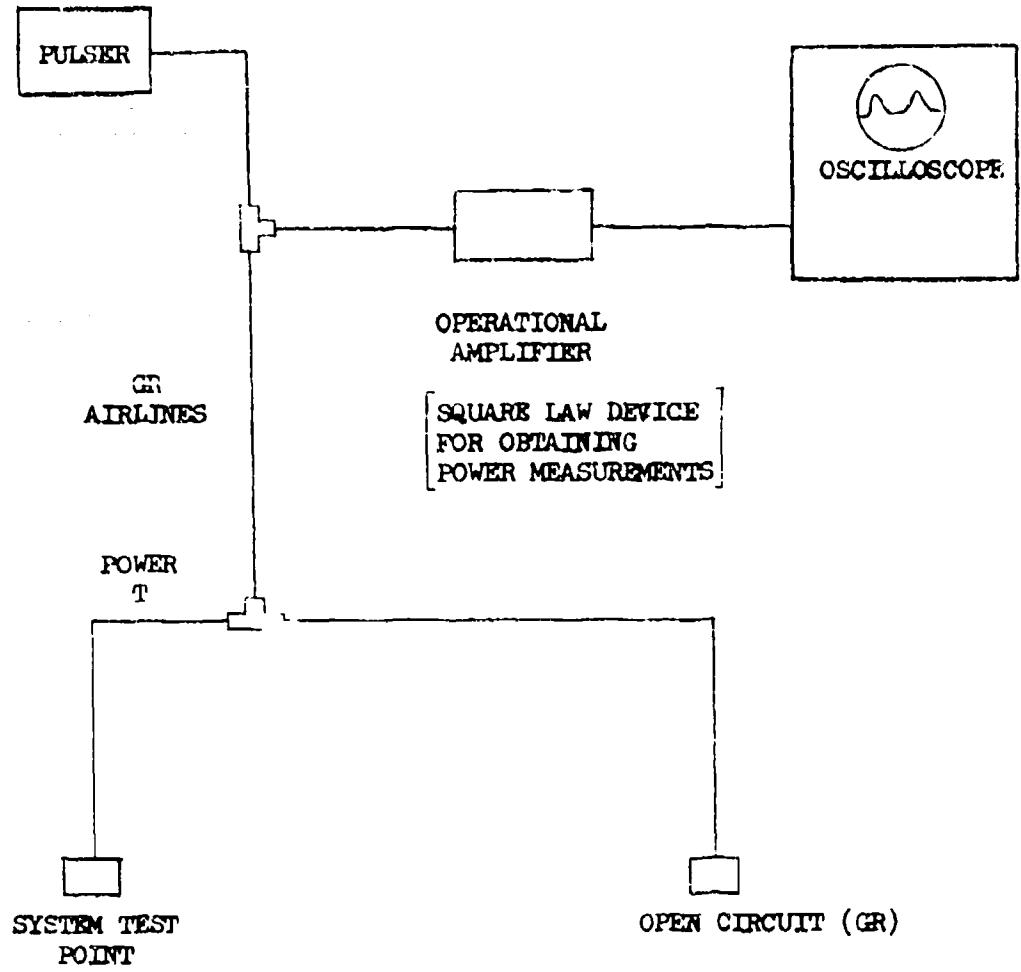


FIG. 2. Pulse Measurement Block Diagram

According to the transmission line theory reviewed in the Theory Section, it should be possible to make all of these measurements from one point in the line by observing the injected pulse and its reflections. Some success has been achieved using only this one circuit connection as shown in Fig. 3.



GR = General Radio

FIG. 3. Single Point Measurement Block Diagram

The initial pulse and the reflected pulse, when observed at the same point, are separated in time by that time period necessary for the pulse to travel down the line and to return. By adding a second line coupled by a power $-T$, open circuited for total reflection and the same length as that to the system test point, a reflection of the initial pulse is developed at the power $-T$ at the same time as the pulse reflected from the system test point. This combined pulse is then observed as $(1 + \rho)V_{IN}$, or MV_{IN} , which is the exact pulse being transmitted past the system termination into the system itself. Thus, the test circuit of Fig. 3 allows a simple measurement of the effectiveness of a protective device in preventing pulse energy from reaching sensitive components within a system without the necessity of probing into the system.

The evaluation of a protective device is normally made using the circuit of Fig. 2. The attenuators after the test device are to reduce amplitude for oscilloscope recording. Those between the pulse generator and the test device are used to vary the initial rate of voltage rise. Since most of the devices evaluated operate on this initial slope, variation of this parameter is needed for full device characterization. A typical set of data showing the voltage amplitude and time required to fire a spark gap across a loaded transmission line is shown in Fig. 4. The applied pulses were, from the left side, 8 kV, 4 kV, 2 kV, and 1 kV.



V: 1 kV/cm
 h: 10 ns/cm

Applied pulse amplitude
 (from the left): 8 kV;
 4 kV; 2 kV; and 1 kV

FIG. 4. Voltage Amplitude Vs. Firing Time of Spark Gap

4. RESULTS

A protective device of the shunt type must be able to shunt destructive pulse energy before the sensitive input devices of the equipment are damaged; however, it must also not degrade the normal operation of the system at lower signal levels. Ideally, such a device must have zero insertion loss and must switch to a dead short in zero time upon sensing the arrival of a large EMP induced pulse. Such devices are hard to find, and non-ideal behavior must be expected. The search for devices approaching the requisite characteristics requires measurement of such things as turn-on time (how fast is it?), shunt resistance (how good a short does it provide?), recovery time (how soon can the equipment resume normal functioning?), and post-pulse characteristics (did the pulse damage the protective device?).

Efforts were made to answer all of these questions for several types of devices--zener diodes, four-layer diodes, and silicon control rectifiers, spark gaps, and neon bulbs. The most thorough analysis has been made on the zener diode.

a. Zener Diodes. At small reverse bias, the zener diode appears as a small capacitance when it is used as a shunt device. As the reverse bias is increased to the zener voltage, the equivalent capacitance decreases and the loss component increases, so that the device looks like a short circuit with a series resistance and inductance. The inductive component results primarily from the physical dimensions of the package and leads. Such a device is excellent for limiting the transmitted pulse amplitude to a low value. The effect of the device capacitance at normal line operating conditions presents a major problem; however, there are some applications which could make use of zener diodes as protective devices.

The frequency cutoff of a zener diode shunting a transmission line was calculated and measured for the case of the 1N753A. From the Theory Section,

$$\rho(s) = - \frac{1}{1 + \frac{2 Z_D}{Z_0}}$$

and

$$M(s) = 1 + \rho(s)$$

$$= \frac{1}{1 + \frac{2 Z_D}{Z_0}}$$

Assume a 50 Ω line and a small reverse bias capacitance of 120 pF for the 1N753A.

$$M(s) = \frac{1}{1 + \frac{25}{Z_D}}$$

$$Z_D = \frac{1}{j \omega C}$$

and

$$M(j\omega) = \frac{1}{1 + j(25)(2\pi)(120 \times 10^{-12}) f \text{ (Hz)}}$$

$$= \frac{1}{1 + j(0.01884) f \text{ (MHz)}}$$

For 3 dB loss, $f = 53$ MHz. The experimental value was 45 MHz.

The equivalent shunt capacitance can be reduced by using a smaller diode, but this will reduce the power dissipation capability of the protective diode.

For a given E_{IN} , R_D is the reciprocal of the slope of the line drawn from the origin to the operating point on the device voltage-current characteristic curve. For the case of a diode shunting a transmission line, E_{IN} (a large voltage step) sees the device resistance, R_D , and the line resistance, R_0 , in parallel.

$$R_L = \frac{R_0 R_D}{R_0 + R_D}$$

Since the reflection coefficient at dc is given by:

$$\rho(0) = \frac{R_L - R_0}{R_L + R_0}$$

we can substitute for R_L and obtain

$$\rho(0) = - \frac{1}{1 + 2 \frac{R_D}{R_0}}$$

From measurement of E_{IN} and E_T , we can calculate $\rho(0)$ from

$$E_T = (1 + \rho) E_{IN}$$

From these calculations, we can obtain current and power levels in the device itself. For the case in which $R_0 = 50 \Omega$ and relative dc conditions prevail:

$$\rho(0) = - \frac{1}{1 + \frac{R_D}{25}} = - \frac{25}{R_D + 25}$$

and

$$M(0) = 1 + \rho(0) = \frac{R_D}{R_D + 25}$$

Note that if $R_D \ll 25$, $\rho(0) \approx -1$.

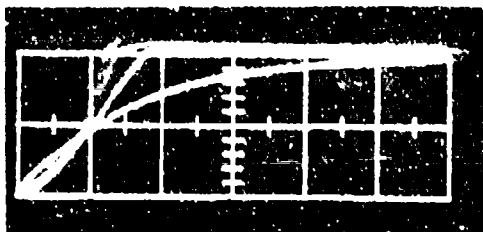
power delivered to the zener diode is then

$$P_D = E_{IN}^2 (1 - \rho^2) \frac{1}{R_D}$$

$$= (1 - \rho^2) P_{IN} \left(\frac{R_0}{R_D} \right)$$

A more thorough analysis would have to include the energy initially stored in the circuit components.

Figure 5 shows the voltage transmitted past a zener diode, 1N3026B, with 18 V zener voltage. Pulses of 160, 80, 40, and 20 V were applied and the responses appear in sequence from the left with diminishing rise times. The larger the input amplitude, the more nearly the E_T rise time matches the E_{IN} rise time.



V: 9.4 V/cm

H: 10 ns/cm

Applied pulse amplitude (from the left): 160 V; 80 V; 40 V; and 20 V.

FIG. 5. Voltage Transmitted Past Zener Diode 1N3026B

b. Four-Layer Diodes/Silicon Controlled Rectifiers. A four-layer diode shunting a transmission line acts like a small capacitor for small signal levels (below device turn-on voltage) and like a small resistor-inductor series combination at large signal levels. Figure 6 shows a sketch of a typical input step and the voltage developed across the diode.

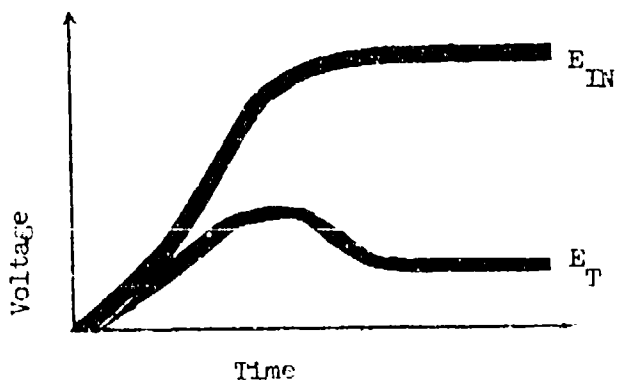
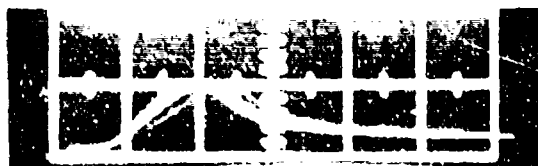


FIG. 6. Input and Transmitted Signals for a Four-Layer Diode

Figure 7 shows a photograph of the E_T curve developed for a 4 kV input pulse. The slower rise time and lower peak amplitude are a result of the device inductance and the input rise time. Following the initial transient portion of E_T , a minimum amplitude is reached for the duration of the input pulse, E_{TN} . This amplitude is related to the equivalent bulk resistance of the device.

A silicon controlled rectifier is basically a four-layer diode with one of the base layers having a contact which can be controlled so that the base acts as a grid. This control allows a wider variety of applications.



V: 500 V/cm

H: 10 ns/cm

FIG. 7. Transmitted Signal for a Four-Layer Diode Shunting a 4 kV Step

c. Spark Gaps. Spark gaps, when properly applied, can provide excellent protection against EMP coupled pulses. Manufacturer's data show the voltage magnitude required to break down the gap (striking voltage) versus response time and initial rate of voltage increase. For example, a gap rated at 230 V as its dc striking voltage may require as much as 1200 V to strike from a ramp voltage applied at the rate of 200 V/ns. Thus, a spark gap with a 230 V dc striking voltage may not adequately protect a circuit which can survive 500 V, because a 1200 V pulse may reach the circuit before the gap fires.

Another problem with spark gaps may occur if a second protective device, such as a zener diode, or a low impedance load is located physically so close to the gap so that the firing voltage is never reached. In such a case, all of the pulse energy goes to the diode or to the load, and damage may occur. Figure 8 shows a line with both a spark gap (Point A) and a low impedance load (Point B) and the voltages present at each point for an input ramp and dc voltage. The voltage developed at Point A is the sum of E_{TN} at Point A, plus E_R from Point B. Thus, the actual voltage developed at Point A may not be as large as the striking voltage, V_G .

In general, if spark gaps are properly used on transmission lines, they should provide protection against large pulses. Figure 9 shows E_T for a spark gap shunting a 50 Ω loaded transmission line. Three values of E_{TN} were used: 8 kV, 4 kV, and 2 kV. The 8 kV pulse was repeated to demonstrate source fluctuation. These data demonstrate the increasing value of striking voltage as E_{TN} increases.

The question of the equivalent resistance of a gap after it has fired can be answered using data from E_T photographs plus information on the input pulse. In order to obtain the dc voltage level across a gap after firing, a slower sweep is employed, as in Fig. 10. Referring back to the Theory Section, we have the following:

Fig. 8a

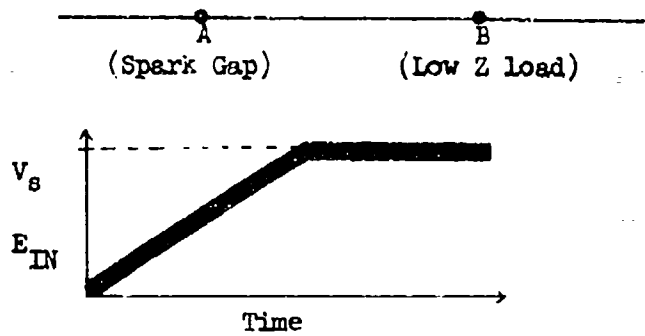


Fig. 8b. Input ramp + dc to Point A

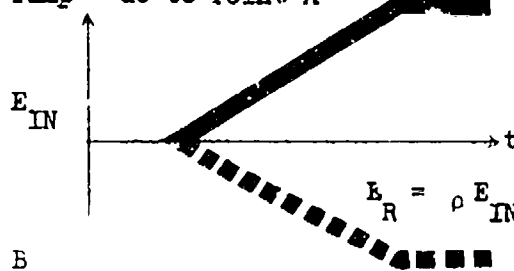


Fig. 8c. Point B

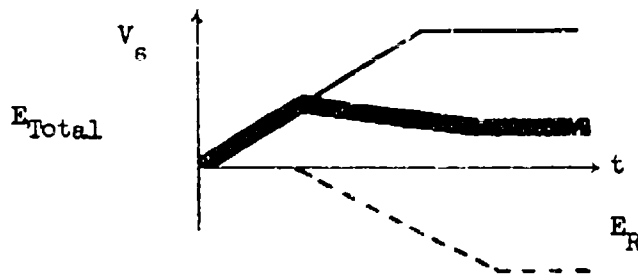


Fig. 8d. Point A

FIG. 8. Spark Gap and Nearby Low Impedance Load

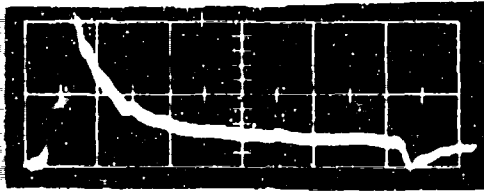


V: 1 kV/cm

H: 10 ns/cm

Input pulse (from the left):
8 kV (2 pulses); 4 kV; and
2 kV

FIG. 9. Transmitted Signal for Spark Gap UBD 550



V: 200 V/cm

R: 20 ns/cm

Input pulse: 8 kV

FIG. 10. Transmitted Voltage for Signalite Spark Gap

$$\begin{aligned}
 E_T &= E_{IN}(1 + \rho) \\
 &= E_{IN} \left(1 + \frac{Z_L - Z_0}{Z_L + Z_0} \right) \\
 &= E_{IN} \left(\frac{2}{1 + \frac{Z_0}{Z_L}} \right)
 \end{aligned}$$

Assuming that the spark gap is across a loaded line,

$$Z_L = \frac{Z_0 Z_D}{Z_0 + Z_D}$$

and

$$\begin{aligned}
 E_T &= E_{IN} \left[\frac{2}{1 + \frac{Z_0}{\frac{Z_0 Z_D}{Z_0 + Z_D}}} \right] \\
 &= E_{IN} \left[\frac{1}{1 + \frac{Z_0}{2 Z_D}} \right]
 \end{aligned}$$

For $Z_0 = 50 \Omega$,

$$\frac{E_T}{E_{IN}} = \frac{1}{1 + \frac{25}{Z_D}}$$

Solving for Z_D :

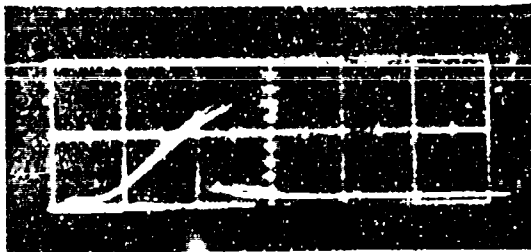
$$Z_D = 25 \left[\frac{1}{\frac{E_{IN}}{E_T} - 1} \right]$$

For this example, $E_{IN} = 8 \text{ kV}$ and from Fig. 10 $E_T = 80 \text{ V}$. Therefore,

$$Z_D = 25 \left[\frac{1}{\frac{8000}{80} - 1} \right] = 25 \left[\frac{1}{99} \right]$$

$$= 0.25 \Omega$$

d. Spark Gap (Special Screw Type). A special spark gap was made by tapping a hole in a General Radio insertion unit and inserting a pointed screw which formed a narrow gap with the center conductor. Under normal signal level operation, this gap appears as a very small capacitor and has negligible effect on the circuit. Application of a high voltage pulse sufficient to fire the gap causes it to shunt the line. Figure 11 shows E_T for several 8 kV E_{IN} pulses. This gap substantially reduces large voltage input pulses, but it appears somewhat inconsistent. The fall time of this pulse is extremely short and may be an important feature.

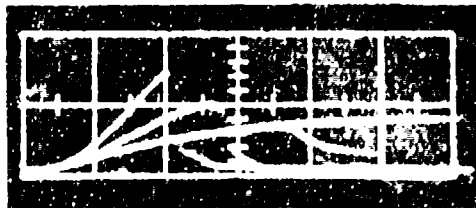


V: 500 V/cm
H: 10 ns/cm

Input pulses: 8 kV

FIG. 11. Transmitted Signal for Special Screw Type Spark Gap.

e. Neon Bulbs. Neon bulbs are similar in operation to spark gaps but have lower dc striking voltages. However, surge striking voltages approach similar values as those of low voltage spark gaps. The advantage of the neon bulb is its very low cost and ready availability. Figure 12 shows the voltage transmitted past a 90 V neon bulb with input pulses of 8 kV, 4 kV, and 2 kV.



V: 2 kV/cm
H: 10 ns/cm

Input pulses (from the left): 8kV,
4 kV, and 2 kV.

FIG. 12. Voltage Transmitted Past 90 V Neon Bulb.

5. CONCLUSIONS

a. Measurement Technique. The technique described allows simple measurements to be performed on military equipment and systems both before and after inclusion of protection devices. These data can be interpreted to determine the system vulnerability to transient effects, such as EMP induced signals in interconnecting cables. The test set-up places the protection device and the protected circuitry in the normal operating configuration. The applied waveform and its reflection are connected at a convenient location in the system and minor parametric variations can be displayed using sampling techniques and a storage oscilloscope. The test system utilizes external calibration standards, thereby eliminating the need for extensive internal set-up procedures. The speed and ease of operation make this a test requiring minimal technical background. With the exception of the high frequency oscilloscope, all components of the test system are readily available or easily constructed. By using a reduced voltage pulse, the normal operation equivalent parameters of a protection device can be determined in the same test set-up.

The technique we have developed and polished over the past two years is simple, easily used by anyone who can operate an oscilloscope, and because all measurements are made in the same set-up which is the actual operating configuration, errors are minimized and confidence enhanced.

b. Protection Device Characteristics. Spark gaps and four-layer diodes exhibited similar properties such as a maximum breakdown voltage of 1400 V with an input pulse of 8 kV amplitude. The transmitted pulse was approximately 30 ns wide, after which the voltage across the device dropped to a low level, determined by the bulk resistance of the device for the duration of the input pulse. Under normal circuit operation, these devices introduced practically no insertion loss.

On the other hand, zener diodes operated at a much lower voltage protection level, but showed large insertion loss under normal operating conditions. In some applications, this could limit their usefulness as protection devices.

We intend to broaden the investigation to include other types of devices with potential protection capability and to identify new approaches to EMP protection involving circuits and materials. The short range goal of this program is to provide protection units for field equipment and equipment in engineering development. The longer range goal is to develop materials, devices, and/or circuits which can be designed into new equipments for the future.

6. ACKNOWLEDGEMENT

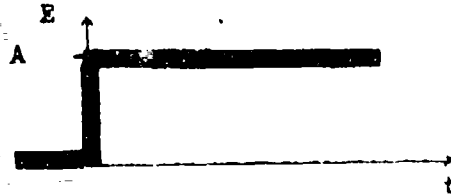
A general note of thanks would be appropriate to Messrs. R. A. Freiberg, G. V. Kedrowsky and M. R. Miller, all of USAFECOM, for many discussions. A particular note of thanks is extended to Mr. G.V. Kedrowsky for his contribution in developing the pulse shaper. Additional thanks are due to Mr. G. Amaro, USAFECOM, for construction of various items.

Partial support was provided by the Defense Nuclear Agency under Contract DR-571.

APPENDIX I. LIST OF SOURCES AND TRANSFORMS

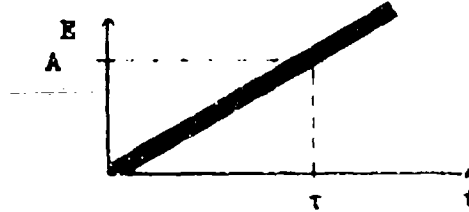
1. Ideal Step

$$E_{IN}(s) = \frac{A}{s}$$



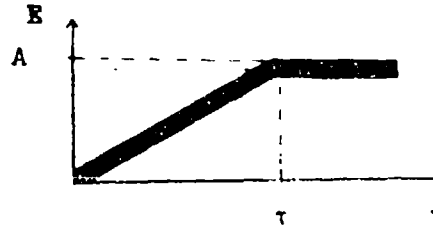
2. Ramp

$$E_{IN}(s) = \frac{A}{\tau} \left(\frac{1}{s^2} \right)$$



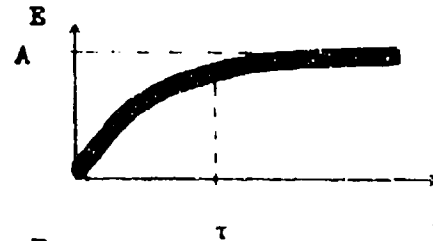
3. Ramp plus dc

$$E_{IN}(s) = \left(\frac{A}{\tau} \right) \left(\frac{1}{s^2} \right) (1 - e^{-s\tau})$$



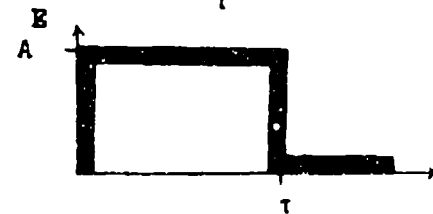
4. Exponential

$$E_{IN}(s) = \left(\frac{A}{\tau} \right) \frac{1}{s(s + \frac{1}{\tau})}$$



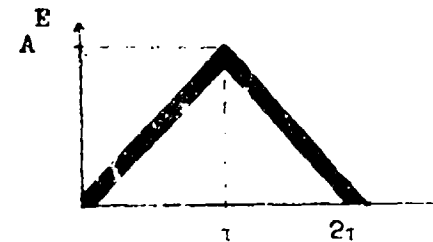
5. Ideal Pulse

$$E_{IN}(s) = A\tau e^{-\frac{1}{2}s\tau} \frac{\sin \frac{\omega\tau}{2}}{\omega \frac{\tau}{2}}$$



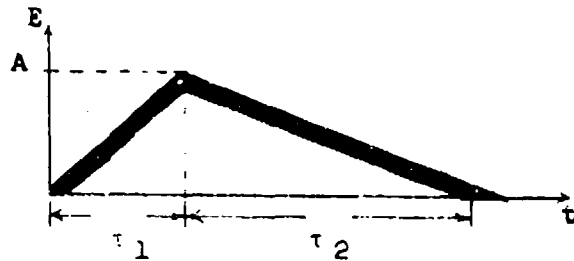
6. Triangular (same slope)

$$E_{IN}(s) = \left(\frac{2A}{\tau} \right) \frac{1}{s^2} \left[e^{\frac{\tau}{2}s} - 2 + e^{-\frac{\tau}{2}s} \right]$$



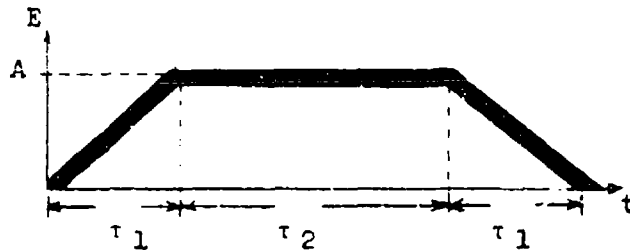
7. Triangular (different slopes)

$$E_{IN}(s) = \left(\frac{1}{s^2}\right) \left[\frac{A}{\tau_1} - \left(\frac{A}{\tau_1} + \frac{A}{\tau_2}\right) e^{-\tau_1 s} + \frac{A}{\tau_2} e^{-(\tau_1 + \tau_2) s} \right]$$



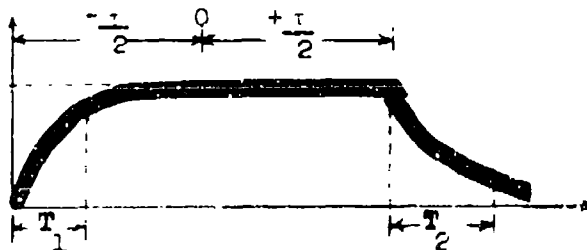
8. Trapezoidal

$$E_{IN}(s) = \left(\frac{A}{\tau_1}\right) \left(\frac{1}{s^2}\right) \left[1 - e^{-\tau_1 s} - e^{-(\tau_1 + \tau_2) s} + e^{-(2\tau_1 + \tau_2) s} \right]$$



9. Pulse with Exponential Rise and Decay

$$E_{IN}(s) = \frac{A}{s} e^{-\frac{\tau}{2}s} - \frac{A}{s + \frac{1}{T_1}} e^{-\frac{\tau}{2}s} - \frac{A}{s + \frac{1}{T_2}} e^{-\frac{\tau}{2}s}$$

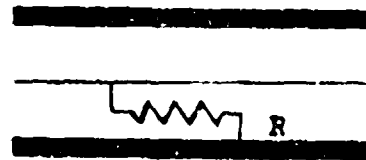


APPENDIX II. LIST OF NETWORK FUNCTION TRANSFORMS
 (Special Case for $Z_0 = 50 \Omega$)

1. Resistor Shunting Line (long line)

$$\rho(s) = \frac{-25}{R + 25}$$

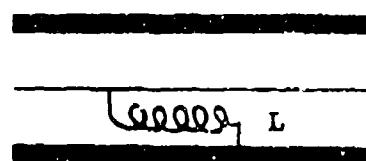
$$M(s) = \frac{R}{R + 25}$$



2. Inductance Shunting Line

$$\rho(s) = \frac{-25}{25 + sL}$$

$$M(s) = \frac{sL}{25 + sL}$$

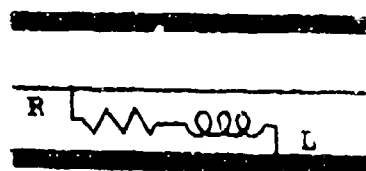


3. Resistor and Inductor in Series Shunting Line

$$\rho(s) = \frac{-25}{R + 25 + sL} = - \left(\frac{25}{L} \right) \frac{1}{s + \frac{1}{T}}$$

$$T = \frac{L}{R + 25}$$

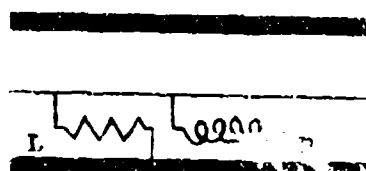
$$M(s) = \frac{R + sL}{R + 25 + sL}$$



4. Resistor and Inductor in Parallel

$$\rho(s) = \frac{-(R + sL)}{R + sL + \frac{RsL}{25}}$$

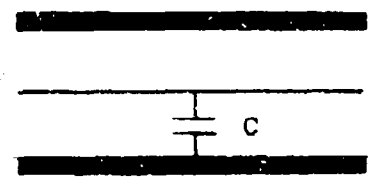
$$M(s) = \frac{\frac{RsL}{25}}{R + sL + \frac{RsL}{25}}$$



5. Capacitor Shunting Line

$$\rho(s) = \frac{-1}{1 + (\frac{1}{25}) Z_c} = \frac{-s}{s + \frac{1}{25C}}$$

$$M(s) = \frac{+\frac{1}{25C}}{s + \frac{1}{25C}}$$

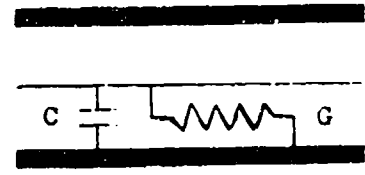


6. Resistor and Capacitor in Parallel Shunting the Line

$$\rho(s) = \frac{-G + sC}{G + sC + \frac{1}{25}}$$

$$M(s) = \frac{\frac{1}{25}}{G + sC + \frac{1}{25}}$$

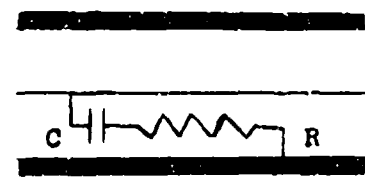
$$G = \frac{1}{R}$$



7. Resistor and Capacitor in Series Shunting Line

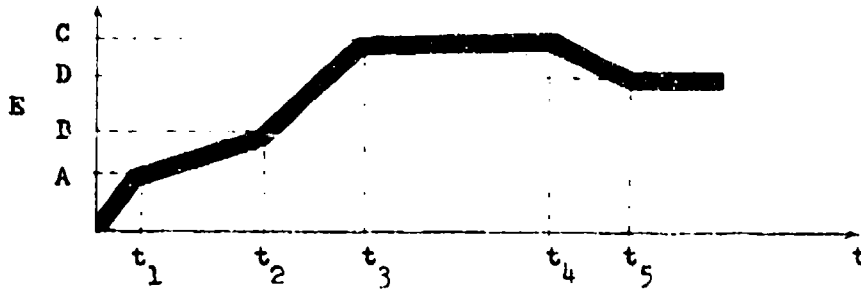
$$\rho(s) = \frac{-sC}{sC + \frac{1}{25} + sCR + \frac{1}{25}}$$

$$M(s) = \frac{\frac{1}{25} + sCR}{sC + \frac{1}{25} + sCR + \frac{1}{25}}$$



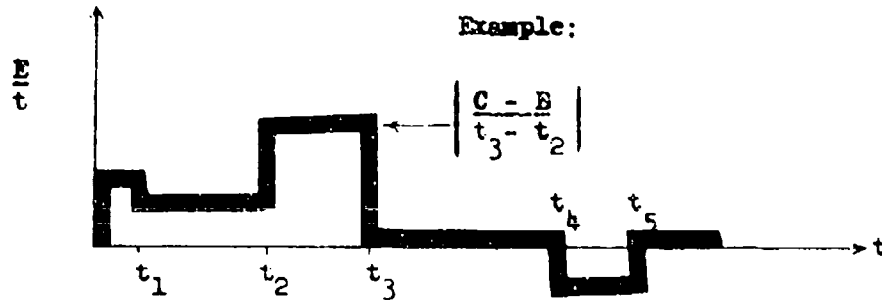
APPENDIX III. Signal Transform by Linear Approximation and Derivatives

Given a signal wave form

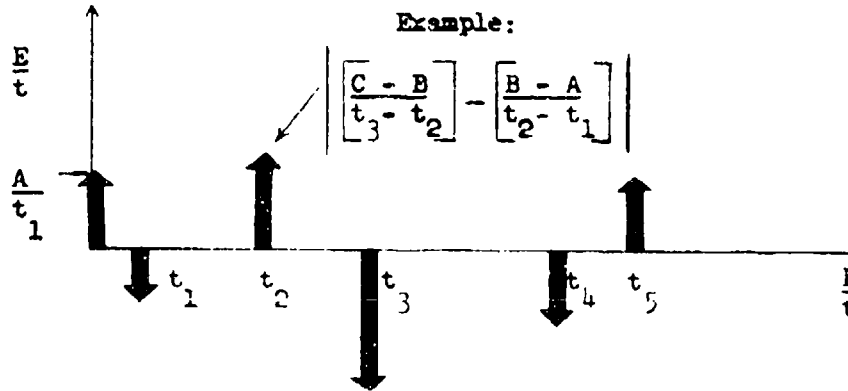


Approximate the signal by piece wise linear function.

Take derivative of piece wise signal

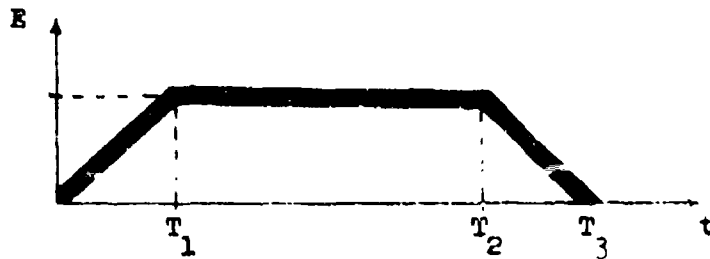


Take second derivative

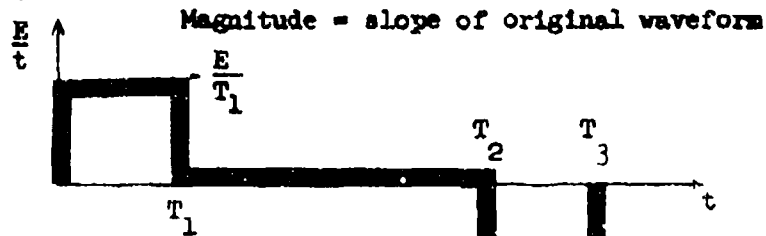


$$f''(t) = \left(\frac{A}{t_1}\right)u(t) - \left[\quad \right] u(t - t_1) + \left[\quad \right] u(t - t_2) + \text{etc.}$$

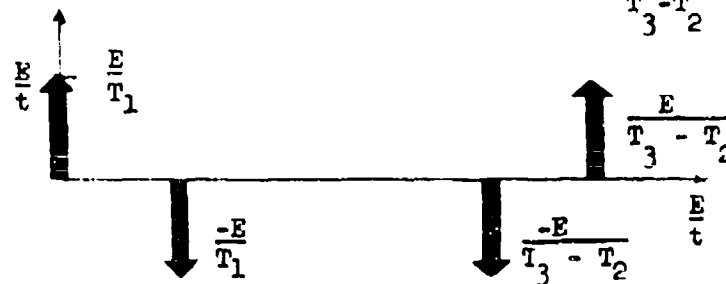
Special example No. 1. Given:



First derivative:



Second derivative:

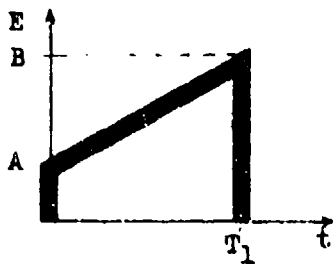


$$f''(t) = \frac{E}{T_1} u(t) - \frac{E}{T_1} u(t - T_1) - \frac{E}{T_3 - T_2} u(t - T_2) + \frac{E}{T_3 - T_2} u(t - T_3)$$

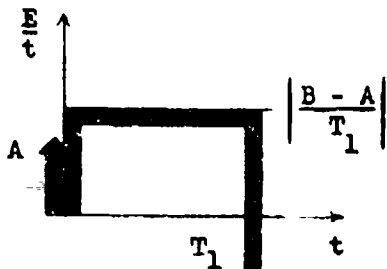
$$s^2 F(s) = \frac{E}{T_1} \left[1 - e^{-sT_1} - \frac{T_3 - T_2}{T_3 - T_2} e^{-sT_2} + \frac{T_3 - T_2}{T_3 - T_2} e^{-sT_3} \right]$$

$$F(s) = \left(\frac{1}{s^2} \right) \left\{ \frac{E}{T_1} \left[1 - e^{-sT_1} \right] - \frac{E}{T_3 - T_2} \left[e^{-sT_2} - e^{-sT_3} \right] \right\}$$

Special example No. 2, involving a doublet. Given:

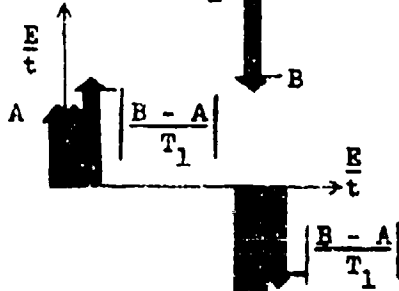


First derivative:



Second derivative:

DOUBLET



$$f''(t) = A \delta'(t) + \frac{B-A}{T_1} \delta(t) - \frac{B-A}{T_1} \delta(t-T_1) - B \delta'(t)$$

$$s^2 F(s) = As + \left(\frac{B-A}{T_1}\right) - \frac{B-A}{T_1} e^{-sT_1} - Bse^{-sT_1}$$

$$F(s) = \frac{A}{s} + \frac{1}{s^2} \left(\frac{B-A}{T_1}\right) - \left(\frac{1}{s^2}\right) \left(\frac{B-A}{T_1}\right) e^{-sT_1} - \frac{B}{s} e^{-sT_1}$$

By using the above procedure, most functions can be quickly and simply approximated.

APPENDIX IV. Equation Solution by Convolution

The reason for the inclusion of the convolution techniques is to provide a method to solve cases where the pulse rise time is not a simple expression (such as the linear or exponential cases) because of cable losses and frequency variations. A graphical technique is then more adaptable to machine analysis.

Equation solution by convolution (for input voltages not analytically expressible): In order to provide a better understanding of rise time effects, the same results can be obtained by graphic convolution.

$$\mathcal{L}^{-1} \left[E_{IN}(s) \cdot v(s) \right] = v(t) * h(t) = \int_0^{\infty} E_{IN}(\tau) h(t-\tau) d\tau$$

where $h(t-\tau)$ is the time shifted impulse response of the network. Also,

$$\mathcal{L}^{-1} \left[sE(s) \cdot \frac{v(s)}{s} \right] = E_{IN}(t) * \int h(t) dt$$

$h(t)$ is the network impulse response.

The equations show that the output time function can be obtained by convolving the input time function with the network impulse response. In addition, the latter equation provides the same information by convolving the derivative of the input time function with the step response of the network.

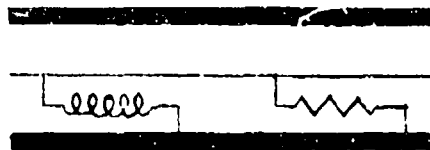
An example of an inductor shunting a 50 ohm transmission line follows:

$$v(s) = - \left(\frac{1}{T} \right) \left(\frac{1}{s + \frac{1}{T}} \right)$$

where $T = \frac{L}{25}$

reflected impulse response

$$E_R(t) = E_{IN} \left(- \frac{1}{T} \right) e^{-\frac{1}{T}t} u(t)$$



*denotes convolution

transmitted impulse response

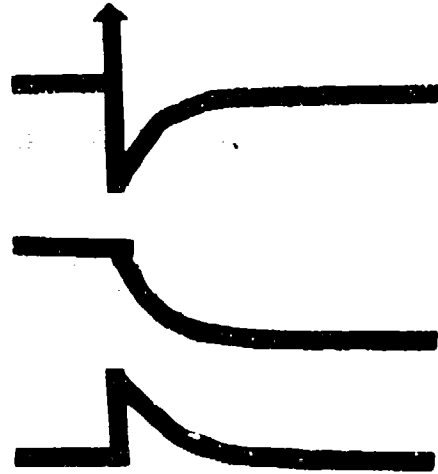
$$E_T(t)_{\delta} = E_{IN} \left[\delta(t) - \left(\frac{1}{T}\right) e^{-\frac{1}{T}t} \right] u(t)$$

reflected step response

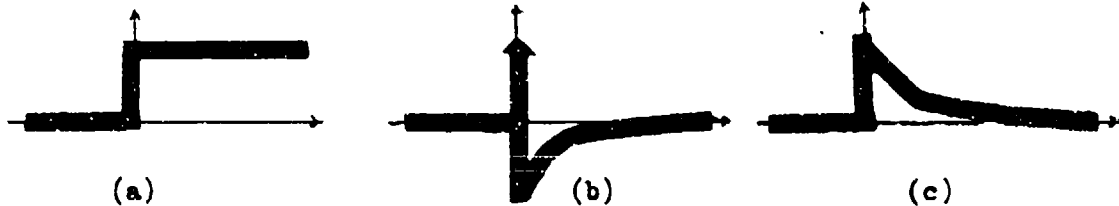
$$E_R(t)_{\square} = E_{IN} (-1) \left[1 - e^{-\frac{1}{T}t} \right] u(t)$$

transmitted step response

$$E_T(t)_{\square} = E_{IN} e^{-\frac{1}{T}t} u(t)$$



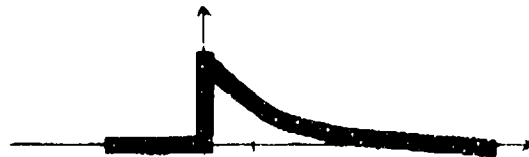
To determine $E_T(t)$ produced by a step function acting on an inductor shunting a transmission line (c), convolute the step function (a) with the impulse response of the network (b)



To convolve two functions graphically, use the reflection of the function about the vertical axis (d) and then shift the function by t (e)

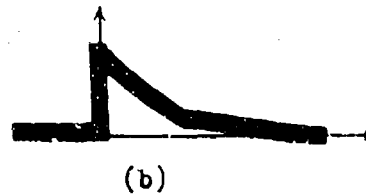
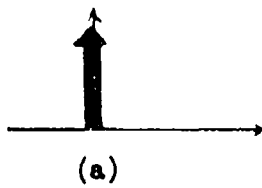


and integrate the product of (e) and (b) for various values of t

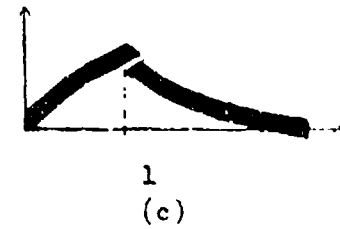
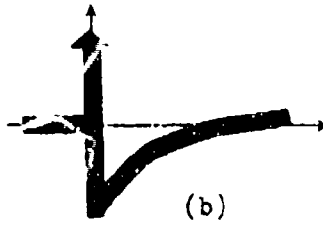
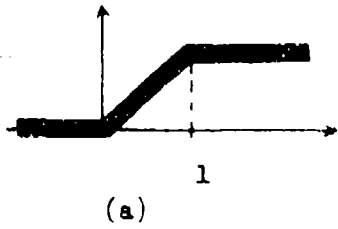


Subscripts δ and \square specify input as the impulse function or step function, respectively.

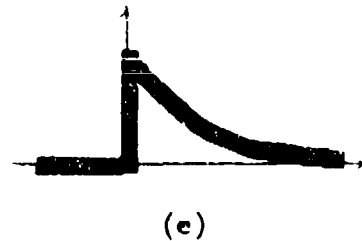
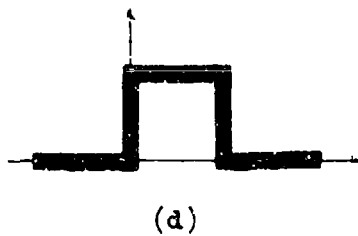
The same result may be obtained by convolving the impulse function (time derivative of step function) (a) with the step response of the network (b).



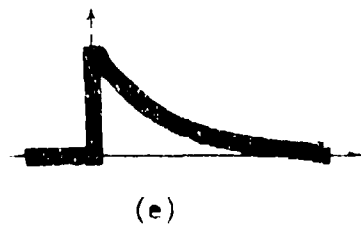
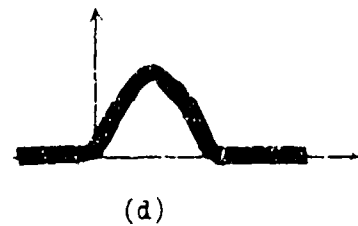
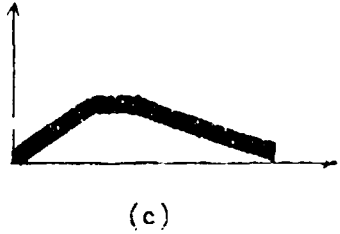
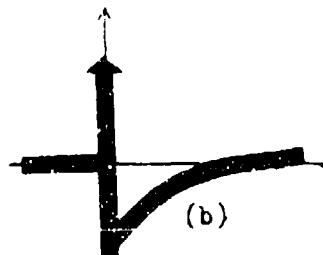
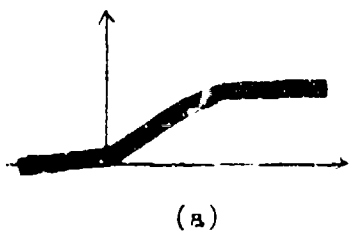
To show the effects of the finite rise time, take the ramp function as the source (a) and convolve it with the network impulse response (b) to get (c)



or the derivative of the input (d) with the step response of the network (e)



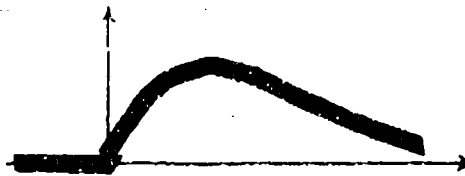
Now, expand the process to non-ideal waves. Convolve (a) with (b) to get (c), or convolve (d) with (e), as above.



If the rise time of the source and detector is fast compared to the network time constant, the source can be represented with a step for a pulse rise and the output is



If the risetime of the pulse is slow, then using an ideal ramp plus dc on the impulse response or a pulse on the step response the output is



Note that the maximum of the convolution integral occurs when

$$t = \tau_1$$

$$E_T(t) = \int_0^{\tau_1} \frac{E_{IN}}{\tau_1} e^{-\frac{1}{T} \tau} d\tau$$

$$T = \frac{L}{25} = \text{Time constant of response}$$

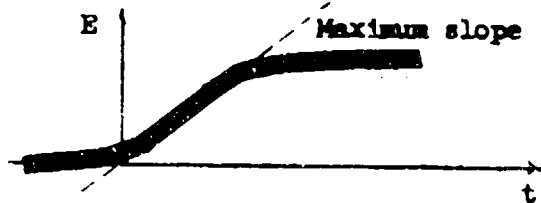
$$\begin{aligned} \left(v_T(t)_{\text{ramp}} \right)_{\text{max}} &= v_T(t)_{\text{max}} = \left(\frac{E}{\tau_1} \right) (-T) \int_0^{\tau_1} \left(\frac{1}{T} \right) e^{-\frac{1}{T} \tau} d\tau \\ &= \left(\frac{E}{\tau_1} \right) (-T) e^{-\frac{1}{T} \tau} \Big|_0^{\tau_1} \\ &= \left(\frac{E}{\tau_1} \right) (-T) \left[e^{-\frac{1}{T} \tau_1} - 1 \right] \\ &= \frac{E}{\tau_1} (T) \left[1 - e^{-\frac{1}{T} \tau_1} \right] \end{aligned}$$

If now $T \gg \tau_1$, then

$$V_T(t) \Big|_{\max} = \left(\frac{E}{L}\right) T = \text{SLOPE} \left(\frac{L}{25}\right) \quad \text{and}$$

$$L = 25 \left[V_T(t) \Big|_{\max} \right] \left[\frac{1}{\text{SLOPE}} \right]$$

The above is generalized to the case



$$L = 25 \left[V_T(t) \Big|_{\max} \right] \left[\frac{1}{\text{MAXIMUM SLOPE}} \right]$$

Appendix V. Example of Measurements and Calculations

This appendix shows impedance calculations made from actual reflection and transmission measurements. The purpose is to summarize the procedures and to show limitations.

1. Figure V-1 shows the reflection measuring circuit (a), the storage oscilloscope display (b), and trace identification guide (c) for the first set of measurements.

For the open circuit case, except for line losses,

$$E_R = \rho E_{IN} \quad \text{and} \quad \rho = \frac{Z_L - Z_0}{Z_L + Z_0} \approx 1$$

so that $E_R \approx E_{IN}$. Similarly, for the short circuit case,

$$\rho = \frac{Z_L - Z_0}{Z_L + Z_0} = -1$$

and $E_R = -E_{IN}$.

For the resistive shunt (case 3 in Fig. V-1), using an 11 Ω resistor, and reading E_R and E_{IN} at some point on the stable, relatively flat portion of the curves, we obtain

$$\rho = \frac{E_R}{E_{IN}} = \frac{-280 \text{ mV}}{420 \text{ mV}} = -0.667$$

but

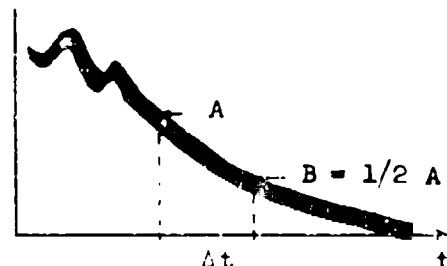
$$\rho = \frac{R - 50}{R + 50} = -0.667$$

and solving for R, $R = 10 \Omega$. This is within 10%.

For the resistive plus inductive series shunt (case 2 of Fig. V-1), using an 11 Ω resistor and a 0.22 μ H inductor, measure the time constant as follows:

Pick a point on the decay curve where the curve has smoothed out (A) and measure the time increment from that point to a point (B) which is 50% of the amplitude at point (A). The time constant is then

$$\frac{\Delta t}{0.69}$$



From Fig. V-1, the time constant of curve 2 is approximately $\frac{4 \text{ ns}}{0.69}$
so that $L = \frac{4 \text{ ns}}{0.69} \times (50 \Omega + 10 \Omega) = 0.34 \mu\text{H}$.

This value is about 50% high, but the accuracy of this technique is greatest when the time constant is much greater than the pulse rise time. In this example, the pulse rise time is approximately $\frac{3 \text{ ns}}{0.69}$ which is close to the observed circuit time constant of $\frac{4 \text{ ns}}{0.69}$.

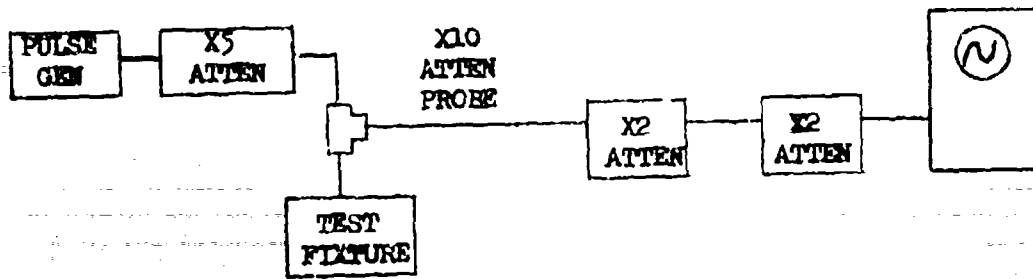


Fig. V-1 (a)



Fig. V-1 (b)

Test Fixture

- | | | |
|---|--|-------|
| 1 | Open circuit | |
| 2 | $11\ \Omega + 0.22\ \mu\text{H}$
Series Shunt | ———— |
| 3 | $11\ \Omega$ Shunt | //// |
| 4 | Short circuit | //// |

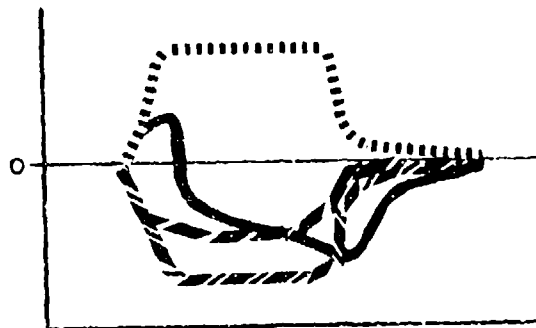


Fig. V-1 (c)

Fig. V-1. Reflection Measurements on Inductive and Resistive Shunts

2. Figure V-2 shows the transmission measuring circuit (a), the storage oscilloscope display (b), and trace identification guide for this set of measurements.

In the open circuit case (curve 1 in Fig. V-2),

$$\begin{aligned} E_2 &= (1 + \rho) E_{IN} = 2 E_{IN} \\ &= 600 \text{ mV} \end{aligned}$$

Therefore, for comparison purposes, $E_{IN} = 300 \text{ mV}$. (The attenuation factors would have to be considered for absolute values of E_{IN} and E_T .)

In the resistive shunt case (curve 3 of Fig. V-2),

$$E_T = (1 + \rho) E_{IN} = \left(1 + \frac{R - Z_0}{R + Z_0}\right) E_{IN}$$

and

$$\frac{E_T}{E_{IN}} = 1 + \frac{R - Z_0}{R + Z_0}$$

$$\text{Substituting values, } \frac{110 \text{ mV}}{300 \text{ mV}} = 1 + \frac{R - 50 \Omega}{R + 50 \Omega}$$

Solving for R, $R = 11.2 \Omega$, within 2%.

For the $0.22 \mu\text{H}$ inductor (curve 4 in Fig. V-2), the time constant is $\frac{3.0 \text{ ns}}{0.69}$, and $L = \frac{3.0 \text{ ns}}{0.69} \cdot 50 \Omega = 0.22 \mu\text{H}$.

For an $0.11 \mu\text{H}$ inductor (curve 5 in Fig. V-2), the time constant is $\frac{1.6 \text{ ns}}{0.69}$ and $L = \frac{1.6 \text{ ns}}{0.69} \cdot 50 \Omega = 0.12 \mu\text{H}$.

Combining the $0.22 \mu\text{H}$ inductor and 11Ω resistor in series shunt (curve 2 of Fig. V-2), the time constant is $\frac{3.0 \text{ ns}}{0.69}$, and again

$L = 0.22 \mu\text{H}$ and $R = 11.2 \Omega$.

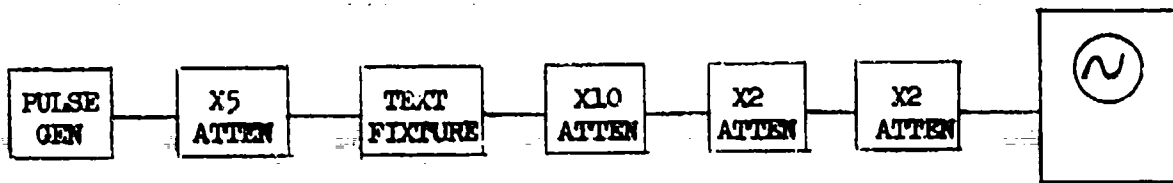


Fig. V-2 (a)

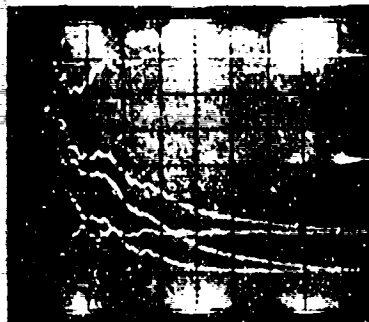


Fig. V-2 (b)

Text Fixture

- | | | |
|---|--|---|
| 1 | Open circuit |  |
| 2 | 11 Ω + 0.22 μ H
Series Shunt |  |
| 3 | 11 Ω Shunt |  |
| 4 | 0.22 μ H Shunt |  |
| 5 | 0.11 μ H Shunt |  |



Fig. V-2 (c)

Fig. V-2. Transmission Measurements on Resistive and Inductive Shunts

3. Figure V-3 shows the transmission measuring circuit (a), the storage oscilloscope display (b), and trace identification guide (c) for this set of measurements.

In the open circuit case (curve 1 in Fig. V-3),

$$E_T = 2 E_{IN} = 600 \text{ mV.}$$

For a 100 pF shunt, the time constant is $\frac{3.6 \text{ ns}}{0.69}$ and $RC = \frac{3.6}{0.69}$.

$$\text{Therefore, } C = \frac{3.6}{0.69} \cdot \frac{1}{50 \Omega} = 104 \text{ pF.}$$

Similarly, for a 47 pF shunt, the time constant is $\frac{1.6 \text{ ns}}{0.69}$ and

$$C = 46 \text{ pF.}$$

However, in the 10 pF case, we again have the situation where the circuit time constant is not long compared to the pulse rise time. Therefore, the calculated value of C is greatly in error.

$$C \sim \frac{0.8 \text{ ns}}{0.69} \cdot \frac{1}{50 \Omega} \sim 23 \text{ pF.}$$

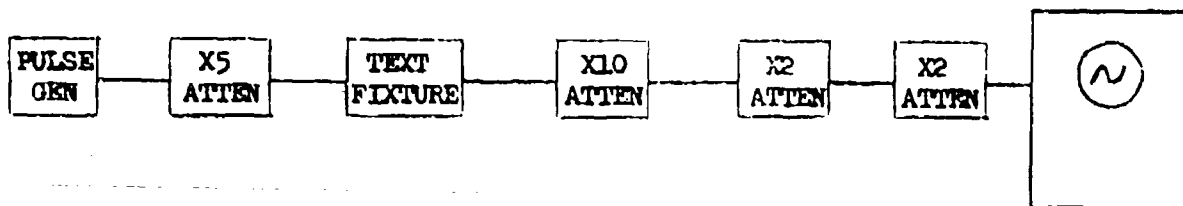


Fig. V-3 (a)

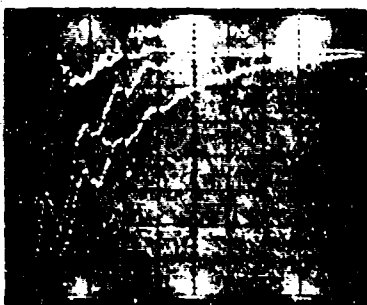


Fig. V-3 (b)

Test Fixture

- 1 Open circuit
- 2 10 pF Shunt
- 3 47 pF Shunt
- 4 100 pF Shunt



Fig. V-3 (c)

Fig. V-3. Transmission Measurements on Capacitive Shunts

Reproduced from
best available copy.

4. Figure V-4 shows the reflection measuring circuit (a), the storage oscilloscope display (b), and trace identification guide (c) for this set of measurements.

For the 100 pF shunt (curve 3 in Fig. V-4), the time constant is $\frac{3.6 \text{ ns}}{0.69}$, and $C = 10^4 \text{ pF}$.

For the 47 pF shunt, the time constant is $\frac{1.8 \text{ ns}}{0.69}$, and $C = 52 \text{ pF}$.

For the 10 pF shunt, the time constant is $\sim \frac{0.6 \text{ ns}}{0.69}$, and $C \sim 17 \text{ pF}$.

As was indicated in paragraph 3 above for the 10 pF case, the time constant is not sufficiently greater than the pulse rise time to make the calculation valid.

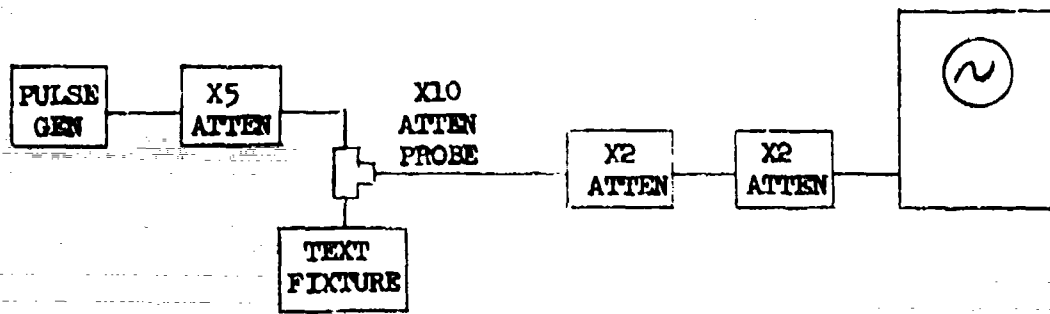


Fig. V-4 (a)

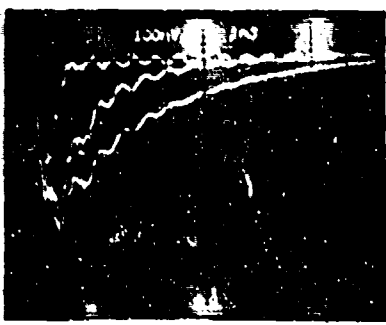


Fig. V-4 (b)

Test Fixture

- 1 10 pF Shunt
- 2 47 pF Shunt
- 3 100 pF Shunt

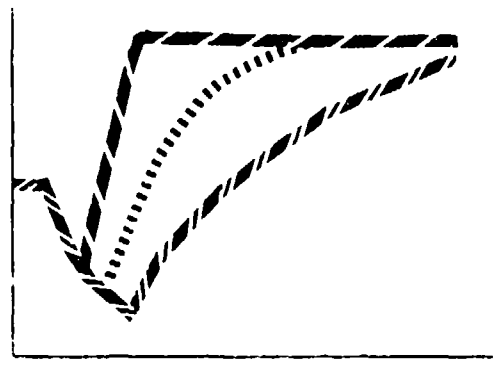


Fig. V-4 (c)

Fig. V-4. Reflection Measurements of Capacitive Shunts (Unloaded Line)

5. Figure V-5 shows the reflection measuring circuit (a), the storage oscilloscope display (b), and trace identification guide (c) for this set of measurements

For the 100 pF case (curve 3 in Fig. V-5), the time constant is $\frac{1.8 \text{ ns}}{0.69}$ and $C = \frac{1.8 \text{ ns}}{0.69} \cdot \frac{1}{\frac{R}{2}} = 104 \text{ pF}$.

For the 47 pF case, the time constant is $\frac{1.2 \text{ ns}}{0.69}$ and $C = 70 \text{ pF}$.

For the 10 pF case, the time constant is $\sim \frac{0.4 \text{ ns}}{0.69}$ and $C \sim 23 \text{ pF}$.

The loading of the line makes RC, the time constant, smaller and now, even the 47 pF case is in error as well as the 10 pF case.

As can be seen from the previous examples, there are two basic limitations to measurements of this type. First, the pulse rise time must be significantly less than the impedance time constant. Second, pulse distortions can make it difficult to read values from the photographs. A particular distortion is the minor oscillation introduced by transmitting the signals over long cables. Some of these limiting difficulties can be avoided by using the component substitution method discussed previously in the text.

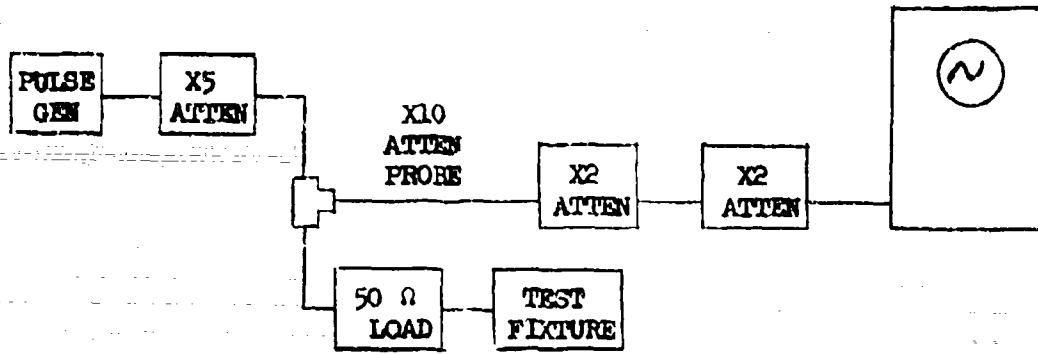


Fig. V-5 (a)

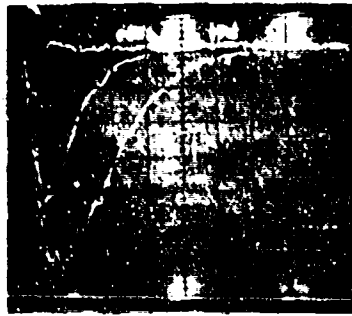


Fig. V-5 (b)

Test Fixture

- 1 10 pF Shunt
- 2 47 pF Shunt
- 3 100 pF Shunt

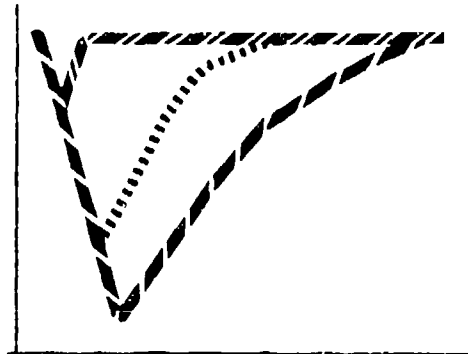


Fig. V-5 (c)

Fig. V-5. Reflection Measurements of Capacitive Shunts (Loaded Line)